The EMBO Journal Vol.17 No.21 pp.6377–6384, 1998

The NMR structure of *Escherichia coli* ribosomal protein L25 shows homology to general stress proteins and glutaminyl-tRNA synthetases

Matthias Stoldt, Jens Wöhnert, Matthias Görlach and Larry R.Brown[1]

Abteilung Molekulare Biophysik/NMR Spektroskopie, Institut für Molekulare Biotechnologie e. V., Postfach 100813, 07708 Jena, Germany

[1]Corresponding author

The structure of the *Escherichia coli* ribosomal protein L25 has been determined to an r.m.s. displacement of backbone heavy atoms of 0.62 ± 0.14 Å by multi-dimensional heteronuclear NMR spectroscopy on protein samples uniformly labeled with ^{15}N or $^{15}N/^{13}C$. L25 shows a new topology for RNA-binding proteins consisting of a six-stranded β-barrel and two α-helices. A putative RNA-binding surface for L25 has been obtained by comparison of backbone ^{15}N chemical shifts for L25 with and without a bound cognate RNA containing the eubacterial E-loop that is the site for binding of L25 to 5S ribosomal RNA. Sequence comparisons with related proteins, including the general stress protein, CTC, show that the residues involved in RNA binding are highly conserved, thereby providing further confirmation of the binding surface. Tertiary structure comparisons indicate that the six-stranded β-barrels of L25 and of the tRNA anticodon-binding domain of glutaminyl-tRNA synthetase are similar.

Keywords: NMR spectroscopy/protein structure/ ribosomal protein/ribosome/RNA binding

Introduction

Recently, there has been renewed interest in the structure of ribosomal proteins for several reasons. First, protein biosynthesis is a central step in the realization of genetic information. Given the complexity of the ~2.3 MDa ribosome, recent progress in understanding the structural basis of protein biosynthesis has largely been based on a combination of low resolution methods, e.g. cryo-electron microscopy with three-dimensional image reconstruction together with footprinting, crosslinking experiments and three-dimensional modeling (e.g. Brimacombe, 1995; Frank, 1997; Mueller and Brimacombe, 1997a,b), with high resolution structures obtained by nuclear magnetic resonance spectroscopy (NMR) or X-ray crystallography for ribosomal proteins (for recent reviews see Liljas and Al-Karadaghi, 1997; Ramakrishnan and White, 1998) or fragments of ribosomal RNAs (White *et al.*, 1992; Szewczak *et al.*, 1993; Wimberly *et al.*, 1993; Betzel *et al.*, 1994; Szewczak and Moore, 1995; Fourmy *et al.*, 1996; Correll *et al.*, 1997; Dallas and Moore, 1997; Puglisi *et al.*, 1997; Perbandt *et al.*, 1998). The 5S rRNA constitutes one of the most highly conserved RNA sequences in nature (Specht *et al.*, 1990). It is an essential component of the large ribosomal subunit, and in *Escherichia coli* it is complexed with the ribosomal proteins L5, L18 and L25 (Chen-Schmeisser and Garrett, 1977). Reconstituted 50S ribosomal subunits lacking the 5S rRNA are inactive in protein biosynthesis (Erdmann *et al.*, 1971; Hartmann *et al.*, 1988). The distal end of the E-domain (also referred to as domain IV) of the 5S rRNA, which is directly adjacent to the E-loop binding site for the L25 protein (Douthwaite *et al.*, 1979; Garrett and Noller, 1979; Huber and Wool, 1984; Ciesiolka *et al.*, 1992; Shpanchenko *et al.*, 1996), has been shown to reside in proximity to the peptidyl transferase ring and the GTPase-associated area of the 23S rRNA leading to the suggestion that this domain might play an as yet unidentified role in the process of peptide bond formation (Dontsova *et al.*, 1994; Sergiev *et al.*, 1998).

Secondly, it has become increasingly apparent in recent years that in addition to simple A-form helices, RNA molecules often contain other characteristic structural elements, e.g. stable tetraloops (Shen *et al.*, 1995) or A platforms (Cate *et al.*, 1996), that may play important structural and functional roles. The D and E helices of the D/E domain of 5S rRNA bound a large internal bulge or E-loop which has a tightly packed helical structure of unusual geometry due to the formation of an array of non-canonical base pairs. The (asymmetric) eukaryote E-loop bulge (Wimberly *et al.*, 1993) has a looped out G-residue which contacts the helix in the major groove in a similar fashion to the α-sarcin/ricin loop of the 23S rRNA (Szewczak *et al.*, 1993; Szewczak and Moore, 1995) and constitutes a structure which probably is also similar to domains of potato spindle tuber viroid (PSTV) RNA and the hairpin ribozyme (Shen *et al.*, 1995). In contrast, the (symmetric) eubacterial E-loop bulge, which is the binding site for the L25 protein, lacks the looped out G-residue (Correll *et al.*, 1997; Dallas and Moore, 1997). Given the large number of homologues of both the L25 protein and the 5S rRNA in various organisms, this system potentially provides a rich source of examples of participation of an apparently common RNA structural element in protein–RNA interactions. At present there are very few protein–RNA complexes for which high resolution structures are available and such data for the L25–E-loop complex is therefore of substantial interest.

Finally, there is evidence for the importance of protein–RNA interactions in an increasing variety of biological processes, including signal transduction and regulation of protein synthesis (for a recent review see Siomi and Dreyfuss, 1997). As ancient proteins, ribosomal proteins might be expected to define archetypal protein folds used in RNA binding. For example, structural data on the cold shock domain (CSD) (Newkirk *et al.*, 1994; Schindelin *et al.*, 1994), the ribosomal protein S17 (Jaishree *et al.*,

1996); the RNA-binding domain of ribosomal protein S1 (Bycroft *et al.*, 1997) and the RNA-binding domains of aspartyl-/lysyl-/phenylalanyl-tRNA synthetases (Cavarelli *et al.*, 1993; Onesti *et al.*, 1995; Mosyak *et al.*, 1995) suggest a potential evolutionary relationship between ribosomal proteins, stress proteins and tRNA synthetases. Because sequence homology of families of RNA-binding proteins may be low, the availability of three-dimensional structures can prove crucial to the recognition of such families.

In the present paper we report the NMR solution structure of the L25 protein from *E.coli* and a determination of the protein surface which is involved in binding the E-loop of 5S rRNA. As with other ribosomal proteins, the availability of a high resolution NMR structure for L25 may aid in future efforts to obtain a precise placement of this protein within low resolution models of the ribosome and hence in assessing possible roles of 5S rRNA in protein biosynthesis. L25 shows a new topology for binding of RNA. Interestingly, many of the residues of L25 involved in RNA binding are widely distributed through the amino acid sequence, but are located on a contiguous surface of the protein structure and are among the most highly conserved positions when compared either with the sequences of the related (Gryaznova *et al*., 1996) general stress protein CTC or with equivalent ribosomal proteins from other eubacteria. We suggest that the structure of L25 may constitute a prototype for a new family of RNA-binding proteins which recognize irregular dsRNA bulges related to the ribosomal E-loop. Furthermore, structural comparisons indicate that L25 is related to the tRNA anticodon-binding domain of glutaminyl-tRNA synthetase (GlnRS; Rould *et al*., 1991). This raises interesting questions about evolutionary relationships, even though the present data suggest that L25 and GlnRS probably bind their cognate RNAs in a different fashion.

Table I. Constraints and structural statistics for the 20 best NMR structures of protein L25

Experimental constraints	
Total number of assigned NOEs	2094
Number of distance constraints	1540
intraresidue	209
sequential	409
medium range (residue i to i + j, j = 2...4)	217
long range (residue i to i + j, j > 4)	705
ϕ dihedral angle constraints	47
hydrogen bond constraints	23
Computational statistics[a]	
DYANA target function (Å^2)	0.52 ± 0.08
AMBER energy (kcal/mol)	–1025 ± 45
Residual violations	
NOE distance constraints, sum (Å)	2.96 ± 0.39
NOE distance constraints, max (Å)	0.17 ± 0.05
dihedral angle constraints, sum (degrees)	5.22 ± 2.57
dihedral angle constraints, max (degrees)	2.17 ± 1.05
Structural statistics[a]	
RMSD[b] (Å) to the mean structure (except residues 10–24)	
backbone heavy atoms	0.62 ± 0.14
all heavy atoms	1.14 ± 0.15
RMSD[b] (Å) to the mean structure (core structure[c])	
backbone heavy atoms	0.33 ± 0.07
all heavy atoms	0.81 ± 0.09
ϕ, ψ angles consistent with Ramachandran plots (%)	
allowed regions	96
most favored regions	60

[a]Average value ± standard deviation.
[b]Superposition made for all heavy atoms of residues 3–9 and 25–94.
[c]β-sheets and α-helices.

Results

Structure determination

The ribosomal protein L25 was purified in uniformly ^{15}N and ^{15}N/^{13}C-labeled form from *E.coli* ribosomes (see Materials and methods). For this 11 kDa protein, a nearly complete set of ^{1}H, ^{15}N and ^{13}C NMR assignments (94.5% backbone, 99% side chain CH) was obtained using multidimensional heteronuclear NMR spectroscopy. A series of three- and four-dimensional heteronuclear NOE spectroscopy experiments and a HNCA[H$^{\alpha}$] NMR experiment were used to extract distance and ϕ dihedral angle constraints, respectively. This information was used to calculate and refine the structure of L25 with the FOUND (Güntert *et al.*, 1998), DYANA (Güntert *et al.*, 1997) and AMBER (Weiner *et al.*, 1984) programs using recently described protocols (Ohlenschläger *et al.*, 1998). A summary of the experimental constraints and of the structural statistics for the 20 structures with the lowest DYANA target function is given in Table I. A superposition of these 20 structures, which have been used to characterize the solution structure of L25, is shown in Figure 1.

Structural description

L25 exhibits a compact fold consisting of a six-stranded β-barrel and two α-helices (Figures 1 and 2A). The overall

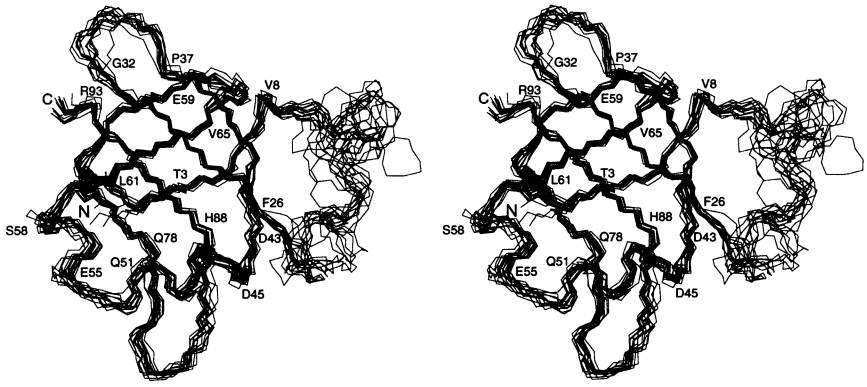

Fig. 1. A stereo view of the ensemble of the 20 NMR solution structures of the L25 protein from *E.coli* with the lowest DYANA target function. The backbone atoms of residues 3–10, 24–31 and 37–94 were used for a least squares superposition of the structures. Only backbone carbon and nitrogen atoms are shown. A ribbon diagram of L25 illustrating the secondary structure elements is given in Figure 2A.

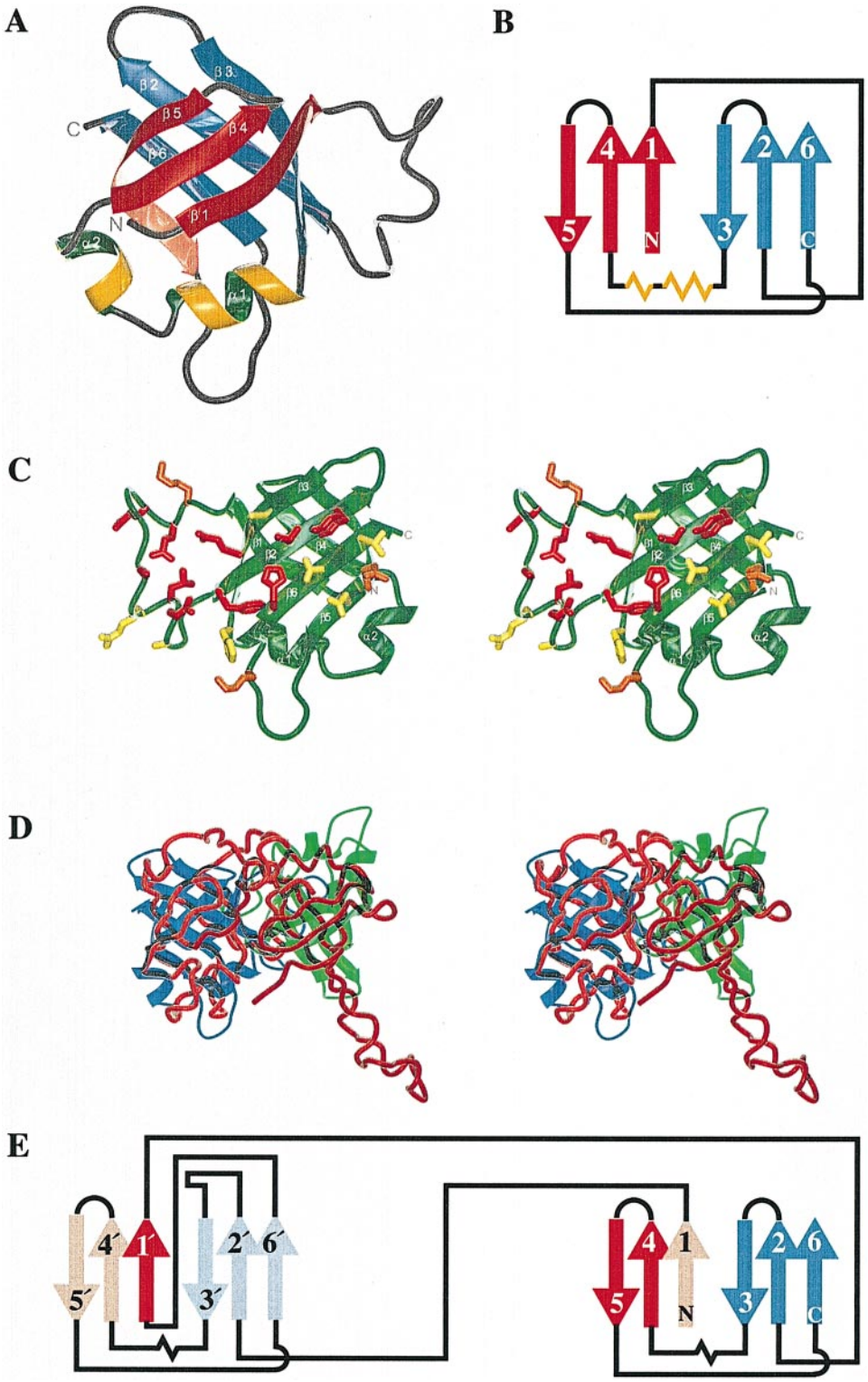

Fig. 2. (**A**) Ribbon diagram of the average L25 structure showing the global fold. The ends of the polypeptide chain (N and C), the β-strands (β1–β6) and the α-helices (α1 and α2) are labeled. (**B**) Topological arrangement of the secondary structural elements of the L25 protein. (**C**) Stereoview of amino acid residues with large ^{15}N chemical shift changes upon binding to 5SE-rRNA represented on a ribbon diagram of the L25 structure. For these residues the heavy-side chain atoms are shown in stick representation. The color code is: yellow for chemical shift changes from 1 to 1.5 p.p.m., orange for changes from 1.5 to 2 p.p.m., and red for changes beyond this limit. Structural elements are labeled as in (A). Relative to (A), the view of L25 is rotated by 180° about a vertical axis in the plane of the page. (**D**) Stereoview of the mean structure of the L25 protein (blue and green ribbon diagrams) superimposed on a tube diagram of the two β-barrels of the anticodon-binding domain of *E.coli* GlnRS (red). (**E**) Topology of the two β-barrels of *E.coli* GlnRS forming the anticodon-binding domain.

shape of the protein is flattened with dimensions of 37×36×22 Å. The connectivity of the secondary structure elements is β1-β2-β3-α1-α2-β4-β5-β6 (Figure 2B). Topologically, the β-barrel shows two repetitions of a motif consisting of two parallel and one antiparallel β-strand (Figure 2B). Either side of the barrel is formed by two

parallel strands, β1 (residues 3–8)/β4 (residues 61–65) and β2 (residues 26–32)/β6 (residues 88–93) and one antiparallel strand, β3 (residues 37–43) and β5 (residues 69–78), respectively (Figures 1 and 2A). The symmetric six-stranded β-barrel is closed by antiparallel β-sheets between strand β1 and the C-terminal residues of strand β3 as well as between strand β6 and the C-terminal residues of strand β5 (Figures 1 and 2A). Strands β3 and β4 are connected by a two-turn α-helix (α1, residues 45–51) and a second one-turn α-helix (α2, residues 55–58) linked to α1 by a short loop of three residues. The axes of the two helices are oriented perpendicularly to each other. Helix α1 closes the bottom of the β-barrel. The short loop between β4 and β5 is well defined (Figure 1), whereas the loops connecting β2/β3 and β5/β6 are somewhat less well defined by the present data. The 17-residue loop between β1 and β2 showed very few NOE contacts to the core of the protein. Nearly half of the backbone amide hydrogens of this loop exchanged very rapidly with the solvent, and $^{15}N\{^{1}H\}$-NOE data for the backbone amides (data not shown) indicated greater motional freedom for this backbone region. This loop, which contains a cluster of positively charged side chains, i.e. two lysines and four out of the six arginine residues, appeared to have limited structural stability in the absence of bound RNA.

Binding of the E-loop of 5S rRNA to the L25 protein

Formation of a complex between L25 and an RNA construct containing the E-loop (Materials and methods) was monitored with a two dimensional ^{1}H-^{15}N HSQC correlation NMR experiment. A 1:1 protein–RNA complex was readily obtained and showed a high quality, very well dispersed ^{1}H-^{15}N HSQC NMR spectrum. Sequential assignments for the backbone amide ^{1}H and ^{15}N resonances were obtained with a three-dimensional HNCA NMR experiment. These experiments also revealed that a number of hydrogens which could not be observed in the free protein due to rapid exchange with solvent, i.e. five arginine NH^{ε} (Arg9, 18, 19, 21, 79) and four backbone amide hydrogens (Lys14, Gly15, Arg18, Leu86), became observable in the RNA–protein complex. This observation suggested that binding to the E-loop of the RNA stabilizes the conformation of the L25 loop residues 9–25 that were poorly defined in the solution structure of the free protein (Figure 1). At the present stage, comparison of the ^{15}N chemical shifts of the L25 backbone amide nitrogens in the free and RNA-bound protein reveals that all substantial changes in chemical shifts are restricted to residues (Lys10 to Gly13, Ser17, Arg19–Ala22, Asn24, Phe26, Ile29 to Tyr31, Ala39, Glu41, His44, Gln75, Asp76, Lys85, His88, Asp90 and Val92) located on one side of the L25 structure (Figure 2C). These results suggest that the lysine/arginine rich loop region (residues 9–25) as well as the surface of β-strands β2 and β6 and the N- and C-terminal residues of β3 and β5, respectively, constitute the regions of L25 involved in binding the cognate E-loop RNA.

Proteins with sequence homology to L25

Comparison of the sequence of L25 to functionally equivalent ribosomal proteins and to a variety of open reading frames in other bacteria reveals that the L25 residues with the most pronounced chemical shift perturbations upon rRNA binding (Figure 2C) show a strong correlation with the most highly, if not absolutely, conserved amino acid sequence positions (Figure 3). In particular, residues in the loop joining strands β1 and β2 (Arg9, Arg18 and Arg21), in β2 (Ile29 and Tyr31) and in β6 (His88 and Asp90), all of which lie in the region implicated as the binding surface for the E-loop on L25, are conserved. Other residues that are conserved (Ala6, Pro27, Ala28, Gly67, Val72, Pro81 and Phe91) appear to have clear roles in maintaining the structure of L25, e.g. Val72 and Phe91 contribute to the hydrophobic core of the β-barrel and Gly67 is involved in the tight loop connecting β4 and β5. On the basis of moderate, pairwise sequence homologies (18–28%; Gryaznova *et al.*, 1996), it has previously been proposed that L25, the functional analogue of L25 in *Thermus thermophilus*, the protein TL5 (Gongadze *et al.*, 1993), and the general stress protein CTC from *Bacillus subtilis* are structurally homologous (Gryaznova *et al.*, 1996). From the structure of L25 and the additional sequence data that have become available recently (Figure 3), it is now apparent that most of the residues that have been implicated in the RNA-binding surface of L25 are conserved in the general stress protein CTC.

Proteins with tertiary structure homology to L25

To search for proteins with similar structural folds to L25, the protein data bank was searched using the DALI server (Holm and Sander, 1993) at the EMBL Heidelberg, Germany. Only one known structure was found to contain the same fold: GlnRS (Rould *et al.*, 1991) from *E.coli* (Figure 2D and E) which is highly related by sequence to GlnRSs from *Haemophilus influenzae* (Fleischmann *et al.*, 1995), yeast (Ludmerer and Schimmel, 1987), the plant lupine [DDBJ/EMBL/GenBank database accession No. X91787, deposited by Siatecka (1995)] and humans (Lamour *et al.*, 1994). In this protein, the anticodon-binding domain of the tRNA synthetase is formed by two β-barrels with an essentially identical topology. These β-barrels are arranged in an antiparallel orientation and each of them shows a high degree of structural similarity to the β-barrel of L25 (Figure 2D and E). For superposition of the backbone heavy atoms of the six β-strands, the r.m.s. displacements between the L25 protein and the two domains of GlnRS are 1.68 and 1.53 Å. However, there is one difference in the overall arrangement of the strands of the β-barrels of L25 and GlnRS, i.e. through topological 'exchange' strand β1 replaces strand β1′ in barrel 2 and vice versa (Figure 2E). Major differences between the two proteins exist both in the length and the orientation of the loops connecting the strands, the occurrence of helices, and additional β-ribbons in the case of GlnRS. The long arginine-rich loop of L25 (residues 9–25) is absent in GlnRS and even within the structurally homologous six-stranded β-barrel, there is very limited sequence homology between the positions constituting the β-barrels of L25 and GlnRS, respectively (Figure 3).

Discussion

Structures containing β-barrels or β-barrel-like motifs are already known for the ribosomal proteins L14 (Davies

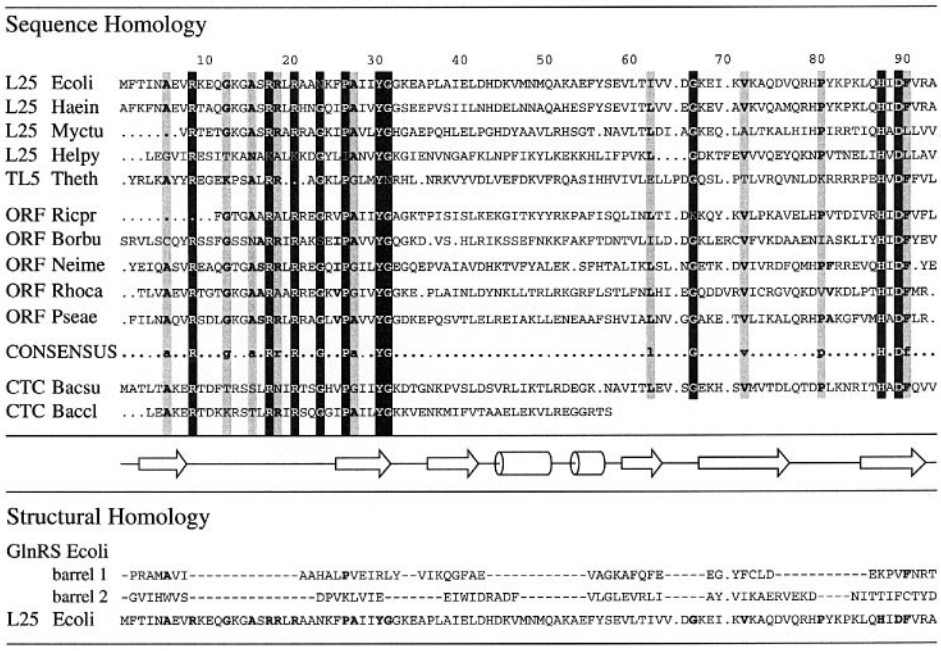

Fig. 3. Top, sequence homology. Alignment and consensus sequence for protein and DNA-derived peptide sequences homologous to L25. The most strongly conserved residues in the 12 sequences are highlighted. White boldface on black background: identical residues for at least ten sequences. Black boldface on grey background: identical residues for eight or nine of the sequences. Note that there are additional positions involving conservative exchanges. Middle, cartoon of β-sheets (arrows) and α-helices (cylinders) found in the NMR structure of protein L25. Bottom, structural homology. Alignment of the structurally analogous β-strand and α-helix sequences of the two β-barrels of *E.coli* GlnRS with *E.coli* protein L25. Sequences were taken from (top to bottom): ribosomal protein L25 from *E.coli* (Bitar and Wittmann-Liebold, 1975); *Haemophilus influenzae* (Fleischmann *et al*., 1995); *Mycobacterium tuberculosis* [DDBJ/EMBL/GenBank database accession No. Z92539, deposited by Murphy *et al*. (1997)]; *Helicobacter pylori* (Tomb *et al*., 1997); and ribosomal protein TL5 from *Thermus thermophilus* (sequence and alignment Gryaznova *et al*., 1996); open reading frames (ORF) from *Rickettsia prowazekii*, *Borrelia burgdorferi* (Fraser *et al*., 1997), *Neisseria meningitidis*, *Rhodobacter capsulatus* and *Pseudomonas aeruginosa* (these sequences were found searching the appropriate on-line databases of these microorganisms, summarized in the TIGR Microbial Database, http://www.tigr.org/tdb/mdb/mdb.html) against the L25 protein sequence; general stress protein CTC from *Bacillus subtilis* (Nilsson *et al*., 1989) and *Bacillus caldolyticus* (fragment) (Krath and Hove-Jensen, 1996); GlnRS from *E.coli* (Hoben *et al*., 1982).

et al., 1996), S1 (Bycroft *et al*., 1997) and S17 (Jaishree *et al*., 1996). However, these are five-stranded with the topology βββββαα (L14), βββαββ (S1) and βββββ (S17). The closed, six-stranded β-barrel of L25 containing four parallel strands and two short α-helices with the topology βββααβββ represents a new fold for ribosomal proteins. This adds a new member to the group of RNA-binding proteins dominated by β-strands which are found in all organisms (Nagai, 1996; Siomi and Dreyfuss, 1997; Varani, 1997).

Protease protection studies on *E.coli* L25 indicated that amino acid residues 1–22 are susceptible to tryptic hydrolysis in the absence of 5S rRNA and that the ΔN22 fragment of L25 lacks RNA-binding activity (Newberry and Garrett, 1980) indicating that the arginine-rich N-terminus is required for binding and/or for the structural integrity of L25. In addition, 1D NMR studies of L25, both free (Kime *et al*., 1981; van de Ven *et al*., 1983) and bound to 5S rRNA, suggested that arginine side-chains play an important role in RNA binding (Kime and Moore, 1984). In the structure presented here this N-terminal region comprises strand β1 and the loop connecting β1 with β2. The backbone amide ^{15}N chemical shift perturbations of L25 upon RNA binding strongly suggest that this loop together with β2 and β6 constitute the major RNA-binding elements of L25 (Figure 2C). However, since small changes of the local geometry and conformation can also lead to chemical shift perturbations upon binding of a ligand (Oldfield, 1995), the residues in the present work which show substantial chemical shift changes may not all be directly interacting with RNA. Conversely, in the case of the RNP motif, mapping of an RNA-binding site on a β-sheet structure via chemical shift changes has proven to be valid (Görlach *et al*., 1992; Oubridge *et al*., 1994; Allain *et al*., 1996). In addition, for the large loop joining strands β1 and β2, which are poorly defined in the solution structure of the free protein (Figure 1), a marked increase in the conformational stability in the RNA–protein complex is indicated by the ^{15}N{^{1}H}-NOEs (data not shown) and by a reduced exchange with solvent observed for the backbone amide hydrogens. This suggests an 'induced fit' type of binding of this loop to RNA. Similarly, in the ribosomal protein L11 an arginine- or lysine-rich loop is flexible in the free protein, but becomes ordered upon binding to its cognate RNA (Hinck *et al*., 1997; Markus *et al*., 1997). On the basis of the present data it appears that L25 may combine two features found for other RNA-binding proteins: the β-sheet region may act as a 'platform' (Görlach *et al*., 1992) which could interact with the flat and broadened minor groove of the central portion of the E-loop while a restructured arginine/lysine-rich loop in turn could fit into the widened major groove (Battiste *et al*., 1996) of the helix IV adjacent to the E-loop. While a full structure of the L25–E-loop complex is clearly still needed, this interpretation of the present data appears to be consistent with a suggested

model of RNA recognition deduced from the structure of E-loop rRNA (Correll *et al*., 1997; Dallas and Moore, 1997).

It has recently been proposed that as ancient proteins, ribosomal proteins may define archetypal folds for groups of now functionally distinct RNA-binding proteins that have evolved from a common ancestor (Bycroft *et al*., 1997). One such family, based on a five stranded β-barrel or a β-barrel-like motif, appears to exist for RNA-binding domains of the type found in the ribosomal protein S1 (Bycroft *et al*., 1997), the ribosomal protein S17 (Jaishree *et al*., 1996), the CSD (Newkirk *et al*., 1994; Schindelin *et al*., 1994) and domains of aspartyl-/lysyl-/phenylalanyl-tRNA synthetases (Cavarelli *et al*., 1993; Mosyak *et al*., 1995; Onesti *et al*., 1995). On the present evidence, it seems that a further such family, based on a six-stranded β-barrel, exists for ribosomal protein L25, general stress protein CTC and GlnRS. The structural data reported here, as well as the elucidation of a corresponding motif for conserved residues which is distributed over the entire protein sequence, suggest that L25 and the general stress protein CTC may recognize similar double-stranded RNA bulge motifs. This information should help in identifying further members of this putative family of RNA-binding proteins. On the other hand, the recognition of the single-stranded anticodon region of tRNA by GlnRS involves a cleft between two six-stranded β-barrels (Rould *et al*., 1991), i.e. an apparently different mode of RNA recognition. The very low level of sequence homology between L25/CTC and GlnRS (Figure 3) might simply reflect the different prerequisites for recognition of irregular dsRNA, i.e. the E-loop rRNA, versus ssRNA, i.e. the tRNA anticodon loop, which may have been acquired through divergent evolution. However, a recent model for the evolution of the glutamyl-/glutaminyl-tRNA synthetase family suggests the acquisition of GlnRS only for a subgroup of the eubacterial kingdom, excluding *Bacillus subtilis* which lacks GlnRS (Ibba *et al*., 1997), via horizontal gene transfer from a eukaryotic source (Lamour *et al*., 1994). Hence, it remains possible that the six-stranded β-barrel, which constitutes a RNA-binding fold for L25 and the anticodon-binding domain of GlnRS, represents a case of convergent evolution.

Materials and methods

Preparation of E.coli L25 samples

Uniformly ^{15}N and $^{15}N/^{13}C$-labeled L25 was purified from an acetic acid extract of 70S polysomes of *E.coli* MRE 600 cells grown in M9 media containing the appropriate isotopes as the sole carbon and/or nitrogen source. Ribosomal proteins were precipitated by acetone fractionation. Proteins from a 65–78% acetone fraction were dissolved in 50 mM sodium phosphate buffer pH 6.5, containing 6 M urea and 4 mM 2-mercaptoethanol, and separated by ion-exchange chromatography on Sepharose Fast Flow (Amersham Pharmacia Biotech). Fractions containing L25 were refolded by dialysis against 50 mM sodium phosphate buffer pH 7.0, containing 0.1 M potassium chloride. L25 was further purified by HPLC on a Mono S HR 5/5 or SOURCE 15S PE 4.6/100 column (Amersham Pharmacia Biotech). Protein samples were concentrated with Centricon-3 concentrators (Amicon, Inc.), and the buffer was exchanged against NMR buffer consisting of 20 mM sodium phosphate pH 7.0, 0.1 M potassium chloride, 3 mM sodium azide and 5% D_2O. Protein concentrations were determined by UV spectrophotometry (ε_{278} =3840 l/mol/cm) to be 1 and 1.4 mM for the ^{15}N and $^{15}N/^{13}C$-labeled NMR samples, respectively. For NMR experiments in D_2O the protein samples were lyophilized and redissolved in 99.996% D_2O (Cambridge Isotopes Laboratories, Inc.).

Preparation of RNA and the protein–RNA complex

A 37 nt oligonucleotide of the sequence 5′-GGACCGAUGGUAGUGUCUUCGGAUGCGAGAGUAGGUC-3′ containing the nucleotides 70–82 and 94–106 of the E-domain of *E.coli* 5S rRNA sequence (5SE-rRNA) was prepared by *in vitro* transcription with T7 RNA polymerase from a linearized plasmid DNA template containing the appropriate sequences including a hammerhead ribozyme directed against the 3′-end of the 5SE-rRNA. ^{15}N-labeled nucleotides were prepared and an optimized 30 ml transcription reaction was carried out essentially as described elsewhere (Grüne *et al*., 1996). Self-cleavage during transcription released the 5SE-rRNA with a uniform 3′-end. The 5SE-rRNA was purified on a DEAE–Sepharose FF column (Amersham Pharmacia Biotech) developed with a sodium acetate step gradient and subsequently by HPLC on a preparative C18 column (Vydac 218TP510) equilibrated with 50 mM potassium phosphate and 2 mM tetrabutylammonium hydrogensulfate, pH 5.9, in water employing an acetonitrile gradient. The product was lyophilized and desalted with a NAP-25 gel-filtration column (Amersham Pharmacia Biotech), precipitated twice with a 5-fold volume of 2% lithium perchlorate in acetone, folded into a monomeric hairpin form by denaturing at 368 K at a concentration of 0.25 mM and subsequent dilution to 0.05 mM with ice cold water and finally exchanged into NMR buffer using Centricon-3 microconcentrators (Amicon, Inc.).

Samples of the protein–RNA complex were prepared in buffer containing 20 mM sodium phosphate, pH 7.2, 0.1 M potassium chloride, 4 mM magnesium chloride, 3 mM sodium azide and 5% D_2O. RNA was added and the titration monitored by 2D ^{1}H-^{15}N HSQC spectra until peaks arising from free protein disappeared, i.e. until a 1:1 complex was obtained.

NMR spectroscopy and spectral assignments

NMR experiments were carried out on a Varian Unity*INOVA* NMR spectrometer operating at 750 MHz proton frequency, at 298 K. Triple resonance NMR spectra used for assignments were processed with the VNMR software (Varian Associates, Inc.). PROSA (Güntert *et al*., 1992) and NmrPipe (Delaglio *et al*., 1995) were used for processing of the 3D NOESY and 4D NOESY spectra, respectively. XEASY (Bartels *et al*., 1995) was employed for visualization and analysis of the spectra. Backbone ^{1}H, ^{13}C and ^{15}N chemical shift assignments were obtained through 3D HNCACB (Wittekind and Mueller, 1993), 3D HNCO (Ikura *et al*., 1990) and 3D CCH-TOCSY-NNH (Grzesiek *et al*., 1993) experiments. Side chain aliphatic ^{1}H and ^{13}C chemical shift assignments were completed by using 3D HCCH-TOCSY-NNH (Grzesiek *et al*., 1993), 3D doubly se-H(C)CH-TOCSY (Sattler *et al*., 1995) and 3D ^{1}H-^{1}H-^{15}N TOCSY-HSQC (Marion *et al*., 1989) experiments. Aromatic resonances were assigned through a selective 3D ^{1}H-^{1}H-^{13}C NOESY-HSQC (Zuiderweg and Fesik, 1989) spectrum (100 ms mixing time). Slowly exchanging amide protons were identified through a ^{1}H-^{15}N HSQC spectrum after dissolving the lyophilized ^{15}N-labeled H_2O NMR sample in D_2O. NOE constraints for structural calculations were obtained from the following experiments: 3D ^{1}H-^{1}H-^{15}N NOESY-HSQC (100 ms mixing time), 3D ^{1}H-^{1}H-^{13}C NOESY-HSQC (80 ms mixing time) selective for aromatic carbons and 3D ^{1}H-^{13}C-^{1}H HSQC-NOESY (80 ms mixing time) selective for aliphatic carbons. Assignment of the ^{15}N-edited NOESY spectrum was assisted by a 4D ^{1}H-^{13}C-^{1}H-^{15}N HMQC-NOESY-HSQC spectrum (Muhandiram *et al*., 1993). Virtually all ^{15}N-edited NOEs as well as ^{13}C-edited NOEs originating from aromatic, H^{α} and resolved methyl groups were assigned manually. Additional NOEs were then automatically assigned using the NOAH algorithm (Mumenthaler *et al*., 1997) as implemented in the DYANA program. $^{3}J_{HNH\alpha}$ vicinal coupling constants for restriction of the ϕ angle were extracted from a 3D HNCA[H^{α}] spectrum (Görlach *et al*., 1993). The $^{1}H^{N}$ and $^{15}N^{H}$ sequential assignments for L25 bound to 5SE-rRNA were obtained from a 3D HNCA experiment (Ikura *et al*., 1990). Heteronuclear $^{15}N\{^{1}H\}$-NOE measurements were made according to the pulse sequence of Kay *et al.* (1989) using the uniformly ^{15}N-labeled protein either free or bound to 5SE-rRNA.

Structure calculation

NOE crosspeak intensities were classified as strong, medium and weak, corresponding to upper distance limit constraints of 2.7, 3.8 and 5.5 Å, respectively. Inter-amide proton NOEs generally were transformed into upper distance limits of 4.4 Å. Dihedral angle constraints were generated by local conformational analysis with the HABAS algorithm (Güntert *et al*., 1991) as implemented in FOUND (Güntert *et al*., 1998) based on $^{3}J_{HNH\alpha}$ vicinal coupling constants and intraresidual and sequential NOEs. Typically, 100 structures were generated by making use of the hybrid distance geometry/simulated annealing protocol of DYANA starting

from random conformations. At the last stage, hydrogen bonds consistently formed in previous calculations were introduced as additional constraints. Out of 100 structures, the 20 with the lowest DYANA target functions were subjected to energy minimization using the AMBER force field (Weiner *et al*., 1984) and used to characterize the solution structure of the L25 protein. Illustrations of protein structures were generated with MOLMOL (Koradi *et al*., 1996).

Acknowledgements

The authors thank A.Figuth for technical assistance in the preparation of isotope-labeled materials, O.Ohlenschläger for help on structural calculations and helpful discussions, and J.Leppert for processing of the four-dimensional NMR spectra. This work was supported by a grant from the Deutsche Forschungsgemeinschaft (Br 1487/2-3). J.W. is grateful to the Fond der chemischen Industrie for financial support.

References

Allain,F.H.-T., Gubser,C.C., Howe,P.W.A., Nagai,K., Neuhaus,D. and Varani,G. (1996) Specificity of ribonucleoprotein interaction determined by RNA folding during complex formation. *Nature*, **380**, 646–650.

Battiste,J.L., Mao,H., Rao,N.S., Tan,R., Muhandiram,D.R., Kay,L.E., Frankel,A.D. and Williamson,J.R. (1996) Alpha helix-RNA major groove recognition in an HIV-1 rev peptide-RRE RNA complex. *Science*, **273**, 1547–1551.

Bartels,C., Xia,T., Billeter,M., Güntert,P. and Wüthrich,K. (1995) The program XEASY for computer-supported NMR spectral analysis of biological macromolecules. *J. Biomol. NMR*, **6**, 1–10.

Betzel,C., Lorenz,S., Fürste,J.P., Bald,R., Zhang,M., Schneider,T.R., Wilson,K.S. and Erdmann,V.A. (1994) Crystal structure of domain A of *Thermus flavus* 5S rRNA and the contribution of water molecules to its structure. *FEBS Lett.*, **351**, 159–164.

Bitar,K.G. and Wittmann-Liebold,B. (1975) The primary structure of the 5S rRNA binding protein L25 of *Escherichia coli* ribosomes. *Hoppe Seylers Z. Physiol. Chem.*, **356**, 1343–1352.

Brimacombe,R. (1995) The structure of ribosomal RNA: a three-dimensional jigsaw puzzle. *Eur. J. Biochem.*, **1**, 365–383.

Bycroft,M., Hubbard,T.J.P., Proctor,M., Freund,S.M.V. and Murzin,A.G. (1997) The solution structure of the S1 RNA binding domain: a member of an ancient nucleic acid-binding fold. *Cell*, **88**, 235–242.

Cate,J.H., Gooding,A.R., Podell,E., Zhou,K., Golden,B.L., Kundrot,C.E., Cech,T.R. and Doudna,J.A. (1996) Crystal structure of a group I ribozyme domain: principles of RNA packing. *Science*, **273**, 1678–1685.

Cavarelli,J., Rees,B., Ruff,M., Thierry,J.C. and Moras,D. (1993) Yeast tRNA (Asp) recognition by its cognate class II aminoacyl-tRNA synthetase. *Nature*, **362**, 181–184.

Chen-Schmeisser,U. and Garrett,R.A. (1977) A new method for the isolation of a 5S RNA complex with proteins L5, L18 and L25 from *Escherichia coli* ribosomes. *FEBS Lett.*, **74**, 287–291.

Ciesiolka,J., Lorenz,S. and Erdmann,V.A. (1992) Structural analysis of three prokaryotic 5S rRNA species and selected 5S rRNA-ribosomal-protein complexes by means of Pb(II)-induced hydrolysis. *Eur. J. Biochem.*, **204**, 575–581.

Correll,C.C., Freeborn,B., Moore,P.B. and Steitz,T.A. (1997) Metals, motifs and recognition in the crystal structure of a 5S rRNA domain. *Cell*, **91**, 705–712.

Dallas,A. and Moore,P.B. (1997) The loop E–loop D region of *Escherichia coli* 5S rRNA: the solution structure reveals an unusual loop that may be important for binding ribosomal proteins. *Structure*, **5**, 1639–1653.

Davies,C., White,S.W. and Ramakrishnan,V. (1996) The crystal structure of ribosomal protein L14 reveals an important organizational component of the translational apparatus. *Structure*, **15**, 55–66.

Delaglio,F., Grzesiek,S., Vuister,G.W., Zhu,G., Pfeifer,J. and Bax,A. (1995) NMRPipe: A multidimensional spectral processing system based on UNIX pipes. *J. Biomol NMR*, **6**, 277–293.

Dontsova,O., Tishkov,V., Dokudovskaya,S., Bogdanov,A., Doring,T., Rinke-Appel,J., Thamm,S., Greuer,B. and Brimacombe,R. (1994) Stem–loop IV of 5S rRNA lies close to the peptidyltransferase center. *Proc. Natl Acad. Sci. USA*, **91**, 4125–4129.

Douthwaite,S. Garrett,R.A., Wagner,R. and Feunteun,J. (1979) A ribonuclease-resistant region of 5S rRNA and its relation to the RNA binding sites of proteins L18 and L25. *Nucleic Acids Res.*, **6**, 2453–2470.

Erdmann,V.A., Fahnestock,K.H. and Nomura,M. (1971) Role of 5S RNA in the functions of 50S ribosomal subunits. *Proc. Natl Acad. Sci. USA*, **68**, 2932–2936.

Fourmy,D., Recht,M.I., Blanchard,S.C. and Puglisi,J.D. (1996) Structure of the A site of *Escherichia coli* 16S ribosomal RNA complexed with an aminoglycoside antibiotic. *Science*, **274**, 1367–1371.

Fleischmann,R.D. *et al.* (1995) Whole-genome random sequencing and assembly of *Haemophilus influenzae* Rd. *Science*, **269**, 496–512.

Frank,J. (1997) The ribosome at higher resolution—the donut takes shape. *Curr. Opin. Struct. Biol.*, **7**, 266–272.

Fraser,C.M. *et al.* (1997) Genomic sequence of a Lyme disease spirochaete, *Borrelia burgdorferi*. *Nature*, **390**, 580–586.

Garrett,R.A. and Noller,H.F. (1979) Structures of complexes of 5S RNA with ribosomal proteins L5, L18 and L25 from *Escherichia coli*: identification of kethoxal-reactive sites on the 5S RNA. *J. Mol. Biol.*, **132**, 637–648.

Gongadze,G.M., Tishchenko,S.V., Sedelnikova,S.E. and Garber,M.B. (1993) Ribosomal proteins, TL4 and TL5, from *Thermus thermophilus* form hybrid complexes with 5S ribosomal RNA from different microorganisms. *FEBS Lett.*, **6**, 46–48.

Görlach,M., Wittekind,M., Beckman,R.A., Mueller,L. and Dreyfuss,G. (1992) Interaction of the RNA-binding domain of the hnRNP C proteins with RNA. *EMBO J.*, **11**, 3289–3295.

Görlach,M., Wittekind,M., Farmer,B.T.,II, Kay,L.E. and Mueller,L. (1993) Measurement of $^{3}J_{HN\alpha}$ vicinal coupling constants in proteins. *J. Magn. Reson.*, **101 (B)**, 194–197.

Gryaznova,O.I., Davydova,N.L., Gongadze,G.M., Jonsson,B.H., Garber,M.B. and Liljas,A. (1996) A ribosomal protein from *Thermus thermophilus* is homologous to a general shock protein. *Biochimie*, **78**, 915–919.

Güntert,P., Braun,W. and Wüthrich,K. (1991) Efficient computation of the three-dimensional protein structures in solution from nuclear magnetic resonance data using the program DIANA and the supporting programs CALIBA, HABAS and GLOMSA. *J. Mol. Biol.*, **217**, 517–530.

Güntert,P., Dötsch,V., Wider,G. and Wüthrich,K. (1992) Processing of multi-dimensional NMR data with the new software PROSA. *J. Biomol. NMR*, **2**, 619–629.

Güntert,P., Mumenthaler,C. and Wüthrich,K. (1997) Torsion angle dynamics for NMR structure calculation with the new program DYANA. *J. Mol. Biol.*, **273**, 283–298.

Güntert,P., Billeter,M., Ohlenschläger,O., Brown,L.R. and Wüthrich,K. (1998) Conformation analysis of protein and nucleic acid fragments with the new grid search algorithm FOUND. *J. Biomol. NMR*, in press.

Grüne,M., Görlach,M., Soskic,V., Klussmann,S., Bald,R., Fürste,J.P., Erdmann,V.A. and Brown,L.R. (1996) Initial analysis of 750 MHz NMR spectra of selectively ^{15}N-G,U labelled *Escherichia coli* 5S rRNA. *FEBS Lett.*, **385**, 114–118.

Grzesiek,S., Anglister,J. and Bax,A. (1993) Correlation of backbone amide and aliphatic side-chain resonances in ^{13}C/^{15}N-enriched proteins by isotropic mixing of ^{13}C magnetization. *J. Magn. Reson.*, **101 (B)**, 114–119.

Hartmann,R.K., Vogel,D.W., Walker,R.T. and Erdmann,V.A. (1988) *In vitro* incorporation of eubacterial, archaebacterial and eukaryotic 5S rRNAs into large ribosomal subunits of *Bacillus stearothermophilus*. *Nucleic Acids Res.*, **16**, 3511–3524.

Hinck,A.P., Markus,M.A., Huang,S., Grzesiek,S., Kustonovich,I., Draper,D.E. and Torchia,D.A. (1997) The RNA binding domain of ribosomal protein L11: three-dimensional structure of the RNA-bound form of the protein and its interaction with 23 S rRNA. *J. Mol. Biol.*, **274**, 101–113.

Hoben,P., Royal,N., Cheung,A., Yamao,F., Biemann,K. and Söll,D. (1982) *Escherichia coli* glutaminyl-tRNA synthetase. II. Characterization of the *glnS* gene product. *J. Biol. Chem.*, **257**, 11644–11650.

Holm,L. and Sander,C. (1993) Protein structure comparison by alignment of distance matrices. *J. Mol. Biol.*, **233**, 123–138.

Huber,P.W. and Wool,I.G. (1984) Nuclease protection analysis of ribonucleoprotein complexes: use of the cytotoxic ribonuclease α-sarcin to determine the binding sites for *Escherichia coli* ribosomal proteins L5, L18 and L25 on 5S rRNA. *Proc. Natl Acad. Sci. USA*, **81**, 322–326.

Ibba,M., Curnow,A.W. and Söll,D. (1997) Aminoacyl-tRNA synthesis: divergent routes to a common goal. *Trends Biochem. Sci.*, **22**, 39–42.

Ikura,M., Kay,L.E. and Bax,A. (1990) A novel approach for sequential assignment of ^{1}H, ^{13}C and ^{15}N spectra of proteins: heteronuclear triple-resonance three-dimensional NMR spectroscopy. Application to calmodulin. *Biochemistry*, **29**, 4659–4667.

Jaishree,T.N., Ramakrishnan,V. and White,S.W. (1996) Solution structure of prokaryotic ribosomal protein S17 by high-resolution NMR spectroscopy. *Biochemistry*, **35**, 2845–2853.

Kay,L.E., Torchia,D.A. and Bax,A. (1989) Backbone dynamics of proteins as studied by ^{15}N inverse detected heteronuclear NMR spectroscopy: application to staphylococcal nuclease. *Biochemistry*, **28**, 8972–8979.

Kime,M.J. and Moore,P.B. (1984) *Escherichia coli* Ribosomal 5S RNA–protein L25 nucleoprotein complex: effects of RNA binding on the protein structure and the nature of the interaction. *Biochemistry*, **23**, 1688–1695.

Kime,M.J., Ratcliffe,R.G., Moore,P.B. and Williams,R.J.P. (1981) A proton NMR study of ribosomal protein L25 from *Escherichia coli*. *Eur. J. Biochem.*, **116**, 269–276.

Koradi,R., Billeter,M. and Wüthrich,K. (1996) MOLMOL: a program for display and analysis of macromolecular structures. *J. Mol. Graphics*, **14**, 51–55.

Krath,B.N. and Hove-Jensen,B. (1996) *Bacillus caldolyticus* prs gene encoding phosphoribosyl-diphosphate synthase. *Gene*, **176**, 73–79.

Lamour,V., Quevillon,S., Diriong,S., N′Guyen,V.C., Lipinski,M. and Mirande,M. (1994) Evolution of the Glx-tRNA synthetase family: the glutaminyl enzyme as a case of horizontal gene transfer. *Proc. Natl Acad. Sci. USA*, **91**, 8670–8674.

Liljas,A. and Al-Karadaghi,S. (1997) Structural aspects of protein synthesis. *Nature Struct. Biol.*, **4**, 767–771.

Ludmerer,S.W. and Schimmel,P. (1987) Gene for yeast glutamine tRNA synthetase encodes a large amino-terminal extension and provides a strong confirmation of the signature sequence for a group of the aminoacyl-tRNA synthetases. *J. Biol. Chem.*, **262**, 10801–10806.

Marion,D., Driscoll,P.C., Kay,L.E., Wingfield,P.T., Bax,A., Gronenborn, A.M. and Clore,G.M. (1989) Overcoming the overlap problem in the assignment of ^{1}H NMR spectra of larger proteins by use of three-dimensional heteronuclear ^{1}H-^{15}N Hartmann–Hahn-multiple quantum coherence and nuclear Overhauser-multiple quantum coherence spectroscopy: application to interleukin 1β. *Biochemistry*, **28**, 6150–6156.

Markus,M.A., Hinck,A.P., Huang,S., Draper,D.E. and Torchia,D.A. (1997) High resolution solution structure of ribosomal protein L11-C76, a helical protein with a flexible loop that becomes structured upon binding to RNA. *Nature Struct. Biol.*, **4**, 70–77.

Mosyak,L., Reshetnikova,L., Goldgur,Y., Delarue,M. and Safro,M.G. (1995) Structure of phenylalanyl-tRNA synthetase from *Thermus thermophilus*. *Nature Struct. Biol.*, **2**, 537–547.

Mueller,F. and Brimacombe,R. (1997a) A new model for the three-dimensional folding of *Escherichia coli* 16 S ribosomal RNA.I. Fitting the RNA to a 3D electron microscopic map at 20 Å. *J. Mol. Biol.*, **271**, 545–565.

Mueller,F. and Brimacombe,R. (1997b) A new model for the three-dimensional folding of *Escherichia coli* 16 S ribosomal RNA. II. The RNA–protein interaction data. *J. Mol. Biol.*, **271**, 545–565.

Muhandiram,D.R., Guang,Y.X. and Kay,L.E. (1993) An enhanced-sensitivity pure absorption gradient 4D ^{15}N, ^{13}C-edited NOESY experiment. *J. Biomol. NMR*, **3**, 463–470.

Mumenthaler,C., Güntert,P., Braun,W. and Wüthrich,K. (1997) Automated combined assignment of NOESY spectra and three-dimensional protein structure determination. *J. Biomol. NMR*, **10**, 351–362.

Nagai,K. (1996) RNA–protein complexes. *Curr. Opin. Struct. Biol.*, **5**, 53–61.

Nilsson,D., Hove-Jensen,B. and Arnvig,K. (1989) Primary structure of the tms and prs genes of *Bacillus subtilis*. *Mol. Gen. Genet.*, **218**, 565–570.

Newkirk,K., Feng,W., Jiang,W., Tejero,R., Emerson,S.D., Inouye,M. and Montelione,G.T. (1994) Solution structure of the major cold shock protein (CspA) from *Escherichia coli*: identification of a binding epitope for DNA. *Proc. Natl Acad. Sci. USA*, **91**, 5114–5118.

Newberry,V. and Garrett,R.A. (1980) The role of the basic N-terminal region of protein L18 in 5S RNA–23S RNA complex formation. *Nucleic Acids Res.*, **8**, 4131–4142.

Ohlenschläger,O., Ramachandran,R., Gührs,K.-H., Schlott,B. and Brown,L.R. (1998) The NMR solution structure of the plasminogen-activator protein staphylokinase. *Biochemistry*, **37**, 10635–10642.

Oldfield,E. (1995) Chemical shifts and three-dimensional protein structures. *J. Biomol. NMR*, **5**, 217–225.

Onesti,S., Miller,A.D. and Brick,P. (1995) The crystal structure of the lysyl-tRNA synthetase (LysU) from *Escherichia coli*. *Structure*, **3**, 163–176.

Oubridge,C., Ito,N., Evans,P.R., Teo,C.-H. and Nagai,K. (1994) Crystal structure at 1.92 Å resolution of the RNA-binding domain of the U1A spliceosomal protein complexed with an RNA hairpin. *Nature*, **372**, 432–438.

Perbandt,M., Nolte,A., Lorenz,S., Bald,R., Betzel,C. and Erdmann,V.A. (1998) Crystal structure of domain E of *Thermus flavus* 5S rRNA: a helical RNA structure including a hairpin loop. *FEBS Lett.*, **429**, 211–215.

Puglisi,E.V., Green,R., Noller,H.F. and Puglisi,J.D. (1997) Structure of a conserved RNA component of the peptidyl transferase centre. *Nature Struct. Biol.*, **4**, 775–778.

Ramakrishnan,V. and White,S.W. (1998) Ribosomal protein structures: insights into the architecture, machinery and evolution of the ribosome. *Trends Biochem. Sci.*, **23**, 208–212.

Rould,M.A., Perona,J.J. and Steitz,T.A. (1991) Structural basis of anticodon loop recognition by glutaminyl-tRNA synthetase. *Nature*, **352**, 213–218.

Sattler,M., Schwendinger,M.G., Schleucher,J. and Griesinger,C. (1995) Novel strategies for sensitivity enhancement in heteronuclear multi-dimensional NMR experiments employing pulsed field gradients. *J. Biomol. NMR*, **6**, 11–22.

Schindelin,H., Jiang,W., Inouye,M. and Heinemann,U. (1994) Crystal structure of CspA, the major cold shock protein of *Escherichia coli*. *Proc. Natl Acad. Sci. USA*, **91**, 5119–5123.

Sergiev,P., Dokudovskaya,S., Romanova,E., Topin,A., Bogdanov,A., Brimacombe,R. and Dontsova,O. (1998) The environment of 5S rRNA in the ribosome: cross-links to the GTPase-associated area of 23S rRNA. *Nucleic Acids Res.*, **26**, 2519–2525.

Shen,L.X., Cai,Z. and Tinoco,I. (1995) RNA structure at high resolution. *FASEB J.*, **9**, 1023–1033.

Shpanchenko,O.V., Zvereva,M.I., Dontsova,O.A., Nierhaus,K.H. and Bogdanov,A.A. (1996) 5S rRNA sugar-phosphate backbone protection in complexes with specific ribosomal proteins. *FEBS Lett.*, **394**, 71–75.

Siomi,H. and Dreyfuss,G. (1997) RNA-binding proteins as regulators of gene expression. *Curr. Opin. Gen. Dev.*, **7**, 345–353.

Specht,T., Wolters,J. and Erdmann,V.A. (1990) Compilation of 5S rRNA and 5S rRNA gene sequences. *Nucleic Acids Res.*, **18** *Suppl.*, 2215–2230.

Szewczak,A.A. and Moore,P.B (1995) The sarcin/ricin loop, a modular RNA. *J. Mol. Biol.*, **247**, 81–98.

Szewczak,A.A., Moore,P.B., Chan,Y.-L. and Wool,I.G. (1993) The conformation of the sarcin/ricin loop from 28S ribosomal RNA. *Proc. Natl Acad. Sci. USA*, **90**, 9581–9585.

Tomb,J.F. *et al.* (1997) The complete genome sequence of the gastric pathogen *Helicobacter pylori*. *Nature*, **388**, 539–547.

van de Ven,F.J.M., de Bruin,S.H. and Hilbers,C.W. (1983) 500-MHz ^{1}H-NMR studies of ribosomal proteins isolated from 70-S ribosomes of *Escherichia coli*. *Eur. J. Biochem.*, **134**, 429–438.

Varani,G. (1997) RNA–protein intermolecular recognition. *Accounts Chem. Res.*, **30**, 189–195.

Weiner,S.J., Kollman,P.A., Case,D.A., Singh,U.C., Ghio,C., Alagona,G., Profeta,S. and Weiner,P. (1984) A new force field for molecular mechanical simulation of nucleic acids and proteins. *J. Am. Chem. Soc.*, **106**, 765–784.

White,S.A., Nilges,M., Huang,A., Brünger,A.T. and Moore,P.B. (1992) NMR analysis of helix I from the 5S RNA of *Escherichia coli*. *Biochemistry*, **31**, 1610–1621.

Wimberly,B., Varani,G. and Tinoco,I.,Jr (1993) The conformation of loop E of eukaryotic 5S ribosomal RNA. *Biochemistry*, **32**, 1078–1087.

Wittekind,M. and Mueller,L. (1993) HNCACB, a high-sensitivity 3D NMR experiment to correlate amide-proton and nitrogen resonances with the α- and β-carbon resonances in proteins. *J. Magn. Reson.*, **101 (B)**, 201–205.

Zuiderweg,E.R. and Fesik,S.W. (1989) Heteronuclear three-dimensional NMR spectroscopy of the inflammatory protein C5a. *Biochemistry*, **28**, 2387–2391.

Received July 17, 1998; revised September 4, 1998; accepted September 7, 1998